Review

CellPress

A matter of scale: how emerging technologies are redefining our view of chromosome architecture

Diego I. Cattoni, Alessandro Valeri, Antoine Le Gall, and Marcelo Nollmann

Centre de Biochimie Structurale, CNRS UMR5048, INSERM U1054, Université de Montpellier, 29 rue de Navacelles, 34090 Montpellier, France

The 3D folding of the genome and its relation to fundamental processes such as gene regulation, replication, and segregation remains one of the most puzzling and exciting questions in genetics. In this review, we describe how the use of new technologies is starting to revolutionize the field of chromosome organization, and to shed light on the mechanisms of transcription, replication, and repair. In particular, we concentrate on recent studies using genome-wide methods, single-molecule technologies, and super-resolution microscopy (SRM). We summarize some of the main concerns when employing these techniques, and discuss potential new and exciting perspectives that illuminate the connection between 3D genomic organization and gene regulation.

The importance of context

In addition to the information encoded in the genetic sequence, chromosomes encompass other channels of information, including epigenetic modifications, regulatory sequences, and spatial organization. These distinct information channels, directly or indirectly, define how the genetic code is interpreted. The spatial organization of genomes influences, and is affected by, many fundamental cellular processes, such as gene expression, DNA repair, DNA replication, and chromosome segregation. Recent technological advances have considerably accelerated our understanding of how chromosomes are organized in the cell, revealing several novel scales of DNA organization, and are starting to unveil the molecular mechanisms involved in this complex organization. In this review, we describe some of the most recent state-of-the-art technologies and discuss how these have been applied to unravel new principles of chromosome organization. In particular, we concentrate on genome-wide, single-molecule, and SRM methods and address their advantages, limitations, and future challenges.

General chromosome organization

The DNA of a eukaryotic cell must be compacted by four orders of magnitude to fit into a micrometer-size nucleus. This is mainly accomplished by the hierarchical folding of DNA. At the lowest level of organization, naked double-stranded DNA is wrapped around an octamer of core histone proteins, which are the primary architectural elements of the chromatin fiber, to form a nucleosome [1]. In eukaryotes, chromosome folding changes dramatically during the cell cycle, with interphase and metaphase chromosomes displaying probably the most well-defined and distinct architectures. During interphase, chromosomes occupy discrete, albeit loose, nuclear regions termed chromosome territories [2,3]. Within territories, chromosome segments adopt complex organizations and topographies depending on their degree of compaction and can be dynamically repositioned to regulate gene expression [4]. Before cell division, a remarkable structural transformation takes place and chromosomes reorganize spatially and converge to a highly condensed mitotic chromosome state adopting a characteristic X-shaped morphology before cytokinesis takes place [5].

Glossary

3C: chromosome conformation capture. Method enabling the determination of interaction frequencies between pairs of genomic loci.
CRISPR-Cas: clustered, regularly interspaced, short palindromic repeat technology. A new approach for generating RNA-guided nucleases that allow for editing, regulating and targeting genomes (more widely defined as RNA-guided engineered nucleases RGENs).
FCS: fluorescence correlation spectroscopy. FCS is a microscopy-based methodology that by correlation analysis of fluorescence intensity fluctuations (in time) of diluted solutions of fluorophores permits the measurement of diffusion coefficients and average concentrations.
FCCS: fluorescence cross-correlation spectroscopy is an extension of the FCS technology that measures the correlation between nonspectrally overlapping fluorophores providing a highly sensitive measurement of molecular interactions.
Genomic 3C: 3C methods allowing for the identification of chromatin interactions across the entire genome (including Hi-C and 3C-seq).
Oligopaint: A PCR-based method for generating highly efficient single-stranded DNA FISH probes from complex DNA libraries. This flexible method enables the visualization of large genomic regions, ranging in size from tens of kilobases to megabases.
PALM: photo-activated localization microscopy and **STORM:** stochastic optical reconstruction microscopy are wide-field fluorescence microscopy imaging methods that rely on the localization of single molecules to achieve spatial resolutions below 20–30 nm.
RICS: raster image correlation spectroscopy measures correlations in space to measure molecular dynamics and concentrations from fluorescence confocal images.
SIM: structured illumination microscopy. Super-resolution imaging technology enabling multicolor, 3D imaging at resolutions of ~100 nm.

Corresponding author: Nollmann, M. (marcelo.nollmann@cbs.cnrs.fr).
Keywords: chromatin structure; chromosome conformation capture; super-resolution microscopy; single molecule microscopy; gene expression.

0168-9525/
 http://dx.doi.org/10.1016/j.tig.2015.05.011

In contrast to eukaryotes, bacteria do not go through a defined interphase period and most DNA processes (e.g., replication, transcription, and repair) occur simultaneously making studies of chromosome folding and regulation more challenging. Bacteria organize their genetic material following a hierarchical organization similar to that observed for eukaryotes: at the lowest level of organization chromosomes are condensed mainly by negative supercoiling and by histone-like, nucleoid-associated proteins (NAPs), while at higher levels they are segmented into micro- (10–20 kbp in sizes, [6]) and macrodomains (hundreds of kbp in size, [7]) that define topological domains and genetic insulation of different chromosomal regions.

Genome-wide methods to study 3D folding of DNA

Chromosome conformation capture (3C; see Glossary) was developed in the early 2000s as a biochemical strategy to analyze the physical contacts between different regions of a chromosome and between the different chromosomes in cell populations [8]. Briefly, 3C methods seize a snapshot of the chromosome conformation at a given moment by crosslinking (by means of chemically fixative agents) DNA segments in close spatial proximity followed by a re-ligation step and PCR amplification or DNA sequencing (Figure 1A). The results obtained are then depicted as frequency contact maps (Figure 1B) representing the probability of two DNA segments being close in space. More recently, the coupling of 3C to high-throughput sequencing [9–11] permitted the detection of genome-wide chromatin interactions and the study of local chromatin folding at scales ranging from tens to hundreds of kilobase pairs with resolutions that have recently reached 2 kbp [12]. Currently, the two most commonly used strategies for genome-wide studies, Hi-C and 3C-seq [10,11], differ in that Hi-C includes a step to introduce biotinylated nucleotides at ligation junctions, enabling their specific purification, whereas in 3C-seq, the digested DNA is re-ligated and directly sequenced without biotin incorporation (Figure 1A). The application of these genomic 3C methods (Hi-C, and 3C-seq and derivatives) led to the discovery of a new level of organization for interphase chromosomes that is characterized by chromosomal regions displaying high frequencies of self-interactions termed physical domains, topologically associating domains (TADs), or topological domains [11,13,14]. In certain cases, TADs correlate with active and repressive chromatin states [11,13–15]. TADs can vary greatly in size, ranging from megabases to hundreds of kilobases depending on the organism (1 Mbp and ~100 kbp in human/mouse and *Drosophila*, respectively [11,14,16]).

Importantly, genomic 3C methods have also been instrumental in the study of the principles and mechanisms regulating gene expression. In human and mouse cells, over 10^5 and 10^6 loops or long-range interactions (LRIs) linking transcription start sites and distal elements were observed [17,18]. By ligating DNA in intact nuclei (*in situ* Hi-C), Rao *et al*. [19] generated much denser Hi-C maps reaching resolutions of ~1 kbp and found a much lower number of interactions for the whole human genome (~10^4 loops). Although there are significant differences in the total number of LRIs, probably associated with the limitations of each method and the lack of standardized data analysis strategies, all of these studies reinforce the previous hypothesis proposing that the main mechanism by which regulatory elements communicate with their cognate target genes is by chromatin looping [20]. Over the past decade, several other genome-wide technologies have been developed that complement well the different 3C methodologies. ChIP-microarray (ChIP-Chip [21]) and ChIP-sequencing (ChIP-PET and ChIP-Seq [22], Figure 1A) allow for the identification of specific protein binding sites, whereas gene expression measurements allow for the differentiation of active or repressed transcription chromatin regions. The combined use of genomic 3C, Chip, and gene expression datasets indicates that loops frequently link promoters and enhancers, correlate with gene activation and are enriched with insulator elements, particularly the insulator binding factor CTCF (CCCTC factor).

Chromosomes are dynamic structures and repositioning of a locus relative to nuclear compartments and other genomic loci can regulate its function. A recent study further unveiled the structure of interphase chromosomes and showed that during replication, timing transition regions (i.e., regions of the chromosome separating early and late replication) share a near one-to-one correlation with TAD boundaries and that early replication is associated with diminished interactions with the nuclear lamina [23]. By combining 5C and Hi-C, Naumova *et al*. [24] shed further light on the two distinct chromosome scaffolds observed before and after replication (i.e., the interphase and mitotic stages of the cell cycle). Interestingly, when evaluating different human cell lines, it was observed that chromosomes differed largely in their compartmental and TADs organizations during interphase, while during mitotic phase all cell types converged to virtually identical homogeneous interaction maps for all chromosomes. These results suggest that during the cell cycle chromosomes alternate between cell type-specific and locus-specific interphase organizations, and puts forward the existence of a universal cell-type and locus invariant mitotic conformation.

Long-range gene regulation may involve epigenetic components including proteins of the Polycomb group. These proteins are organized into nuclear foci (termed bodies) that contain silenced Polycomb-targeted chromatin (i.e., repressed genes). Recently, Sexton *et al*. [11], by employing 3C-seq, revealed the organization of the *Drosophila* embryonic nucleus and found that Polycomb proteins establish long-range contacts between silenced TADs (i.e., chromatin regions marked with the repressive histone H3K27me3, Figure 1B) whereas insulator proteins [e.g., centrosomal protein (CP)190, *Drosophila* homolog of CTCF (dCTCF), and boundary element-associated factor (BEAF)-32; see correlation methods section below] are likely to play a relevant role in separating TADs and eventually in organizing the internal architecture of TADs [11,15,25].

For prokaryotic organisms, studies of chromosome architecture by conformation capture are just starting to emerge. Initial models of global chromosome folding and organization in bacteria have been proposed, but only for a limited number of species [26–28]. Importantly, a recent study revealed the existence of eukaryotic-like TADs in

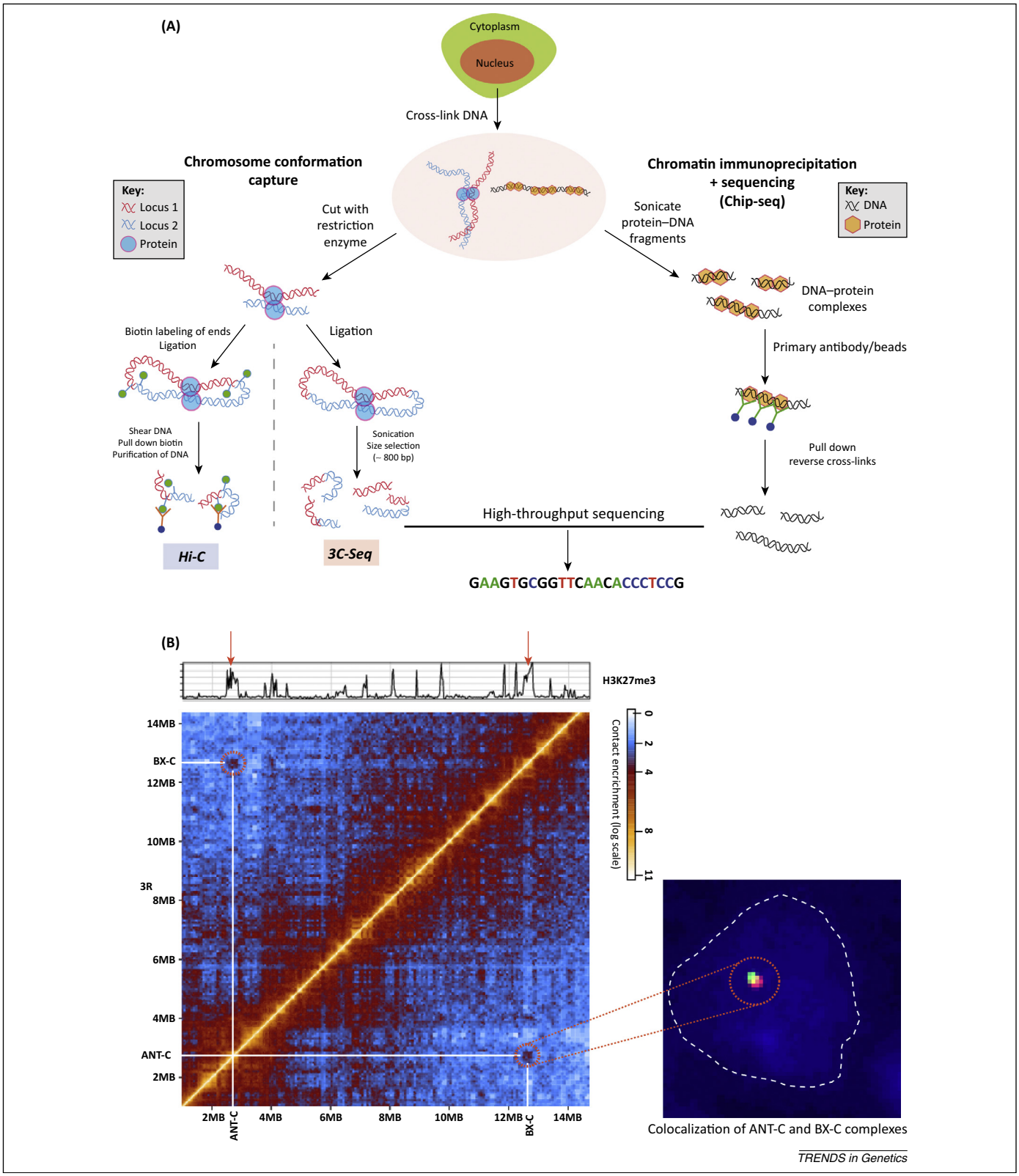

Figure 1. Genome-wide methods to study DNA organization and epigenetic markers. **(A)** Principles of chromosome conformation capture and chromatin immunoprecipitation coupled to sequencing (Hi-C, 3C-Seq, and ChIP-Seq). For genomic 3C experiments (left panel) interacting loci in nuclear DNA are cross-linked with formaldehyde; DNA is then fragmented with restriction enzymes; and staggered DNA ends are either filled (Hi-C) or not (3C-Seq), by using biotinylated nucleotides prior to DNA ligation. For Hi-C experiments, DNA is purified using streptavidin-coated beads, while for 3C-Seq DNA is sonicated and size selected before deep sequencing. For ChIP-Seq experiments (right panel) protein–DNA complexes are cross-linked in the nucleus by formaldehyde fixation. After lysing the cells, DNA is sonicated into 200–1000-bp fragments and protein–DNA complexes immunoprecipitated by probing with a specific antibody. Finally, the cross-links of the protein–DNA complexes are reversed; DNA is further purified and subjected to sequencing analysis. **(B)** 3D folding of the *Drosophila* genome. A normalized 2D heat map of the frequency contact for a 14-Mb region in chromosome 3R is depicted [11]. A linear ChIP-seq profile for the repressive histone H3K27me3 spanning the same region is shown above. Color scale on the right indicates the contact frequency enrichment. The main diagonal observed (intense yellow) in the matrix results from frequent contacts presented by adjacent loci looping onto themselves. Note the long-range contact (highlighted by the red dashed circles) between the two Polycomb-regulated Hox gene clusters ANT-C (Antennapedia complex)

(Figure legend continued on the bottom of the next page.)

Caulobacter crescentus and proposed that domain boundaries are regions displaying high transcriptional activity [29]. Future studies in other well-established bacterial model systems, such as *Bacillus subtilis* and *Escherichia coli*, could ascertain whether TADs are widespread in bacteria, define the mechanisms involved in the formation of bacterial TADs, and determine the role of chromatin folding in other functions such as DNA segregation and replication.

Genomic 3C methods remain technically challenging, and the resolution in the contact maps is limited by the genomic distribution of digestion sites for the specific endonuclease used [30]. To overcome these limitations, the use of DNase was recently proposed for fragmenting cross-linked chromatin combined with DNA-capture technology (DNAase Hi-C), significantly improving the efficiency and coverage of the contact map [12]. Genomic 3C methods, as with other methods such as ChIP and ChIP-Seq, relies on formaldehyde fixation, an empirical and poorly characterized process with variable efficiency capable of introducing several artifacts and false positives [31]. Genomic 3C experiments capture a limited number of all possible interactions in each cell and are performed on a population of tens of millions of cells providing ensemble information of the chromosome conformation, averaging out large, higher-order folding motifs displaying fast dynamics or large cell-state dependence. In addition, the presence of several chromosomes with almost identical genetic content further complicates the precise interpretation of structural models based on genomic 3C data. Overall, structural averaging is particularly important to consider for the interpretation of 3D polymeric models of the chromosome (i.e., the results obtained by modeling assume the existence of a single predominant structure). Recent models have obtained promising results in the study of TAD structures by reproducing conformation ensembles that can predict a range of structural statistical fluctuations of the chromatin fiber [32]. However, it is likely that modeling based on genomic 3C datasets obtained from single-cell technologies using defined biological systems will be needed to achieve accurate structural information.

Recently, a single-cell modified Hi-C strategy was successfully implemented to study the X chromosome of mouse cells [33]. The authors found that TADs are robust and recurrent even at the single-cell level but interdomain contacts are highly variable between individual cells. Additionally, they confirmed that, although there is a range of variability in the large interdomain structure of the X-chromosomal territory, localization of active genes is stably maintained, reinforcing the correlation between chromosome structure and genomic activity. The number of reads attainable in single-cell Hi-C is intrinsically limited by the reduced number of contacts within a single cell and the low efficiency of the enzymatic restriction reaction. Future technological improvements in this method hold great promise, as they will permit the study of cell-to-cell heterogeneity in chromosome structure, allowing for the construction of 3D chromosome conformations from single cells. This is particularly important in achieving the goal of linking chromosome structure to function, such as transcriptional activity.

State-of-the-art microscopy methods to study chromosome organization and dynamics

Single-molecule SRM (smSRM)

For a long time, the microscopic study of the architecture and dynamics of chromosomes has been limited by the resolution attainable by standard fluorescence microscopy. Different methods have been developed over the past two decades to surpass the resolution limit in conventional microcopy (~250 nm). Among them, smSRM methods combine the stochastic photoactivation of a single fluorophore per diffraction-limited volume at any given time and its localization with nanometer spatial resolution. From the coordinates of all localized emitters, a reconstructed image at super-resolution (20–30 nm) can be obtained (Figure 2A). Several smSRM strategies have been designed differing mostly in the fluorescent probe used and the mechanism for achieving stochastic photoactivation, with photo-activated localization microscopy/fluorescence PALM (PALM/fPALM) and stochastic optical reconstruction microscopy/direct STORM (STORM/dSTORM) being the most widely used methods [34–38]. In the following sections, we describe SRM and single-molecule studies investigating DNA structure, transcription, segregation, and repair.

Different labeling approaches can be used to achieve super-resolution imaging of DNA and of factors acting on DNA. A straightforward strategy is to genetically engineer phototransformable fluorescent proteins to tag the factors of interest [39]. This method was used by Cisse *et al*. to label RNA polymerase (Pol II) with dendra2 and study the assembly/disassembly dynamics of transcription factories in human osteosarcoma cells [40]. This important study showed that Pol II does not form static factories, but rather assembles and disassembles dynamic clusters to achieve processive transcription (Figure 2B). Recent studies have used two-color smSRM to study DNA organization and segregation in bacteria. A study by Wang *et al*. [41] characterized the number, size, and distribution of NAP clusters per chromosome in *E. coli* in different growth conditions and showed that operons regulated by the histone-like NAP (H-NS) are preferentially sequestered into these clusters. Recent experiments from the same group revealed an influence of the photoactivatable probe in the formation of H-NS clusters [42], highlighting the importance of using more than one probe to avoid undesired probe clusterization or inhomogeneous density artifacts. Fiche *et al*. [43] revealed that in sporulating *B. subtilis*, the assembly of the DNA motor pump SpoIIIE is cellular-compartment specific and mediated by recognition of specific DNA sequences.

and BX-C (bithorax complex) and the enrichment of the silencing marker H3K27me3 in the Chip-Seq profiles (red arrows) matching the location of these contacts. Bottom right image shows a representative example of the head region of the *Drosophila* embryo cell in which ANT-C and BX-C were fluorescently labeled with two spectrally different fluorophores (red and green) and observed by conventional microscopy. In the head, these two gene groups are silenced by Polycomb proteins, and fluorescently labeled loci colocalize as predicted by the strong signal observed in the contact map (red dashed circles). Blue background in the bottom right image represents DAPI stained DNA and white dotted line denotes the nucleus. Figures in panels (A) and (B) were reproduced, with permission, from [11,96–98].

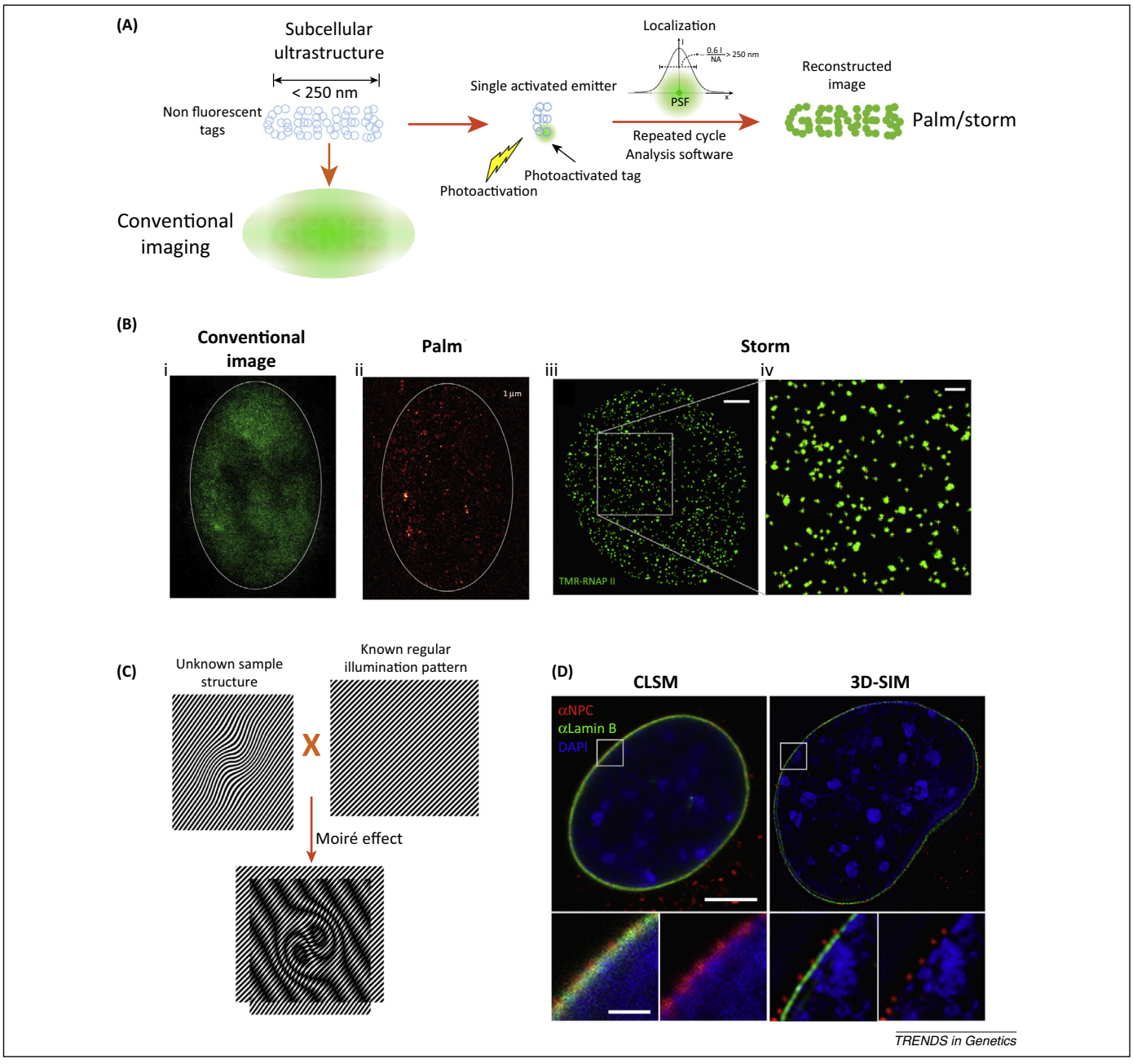

Figure 2. SRM to study chromosomes organization and mechanisms. **(A)** Principles of single-molecule SRM. In a conventional microscopy image of a subcellular structure (left panel) with dimensions smaller than the diffraction limit (~250 nm), all individual fluorophores emit simultaneously and internal structural or dynamical information cannot be resolved (lower left panel). In PALM/STORM fluorophores are in a nonfluorescent state and irradiation with light of the appropriate wavelength induces the stochastic photoactivation of a single fluorophore per diffraction-limited spot (middle panel). Image analysis is used to automatically detect the fluorophore, and its mean position is determined by PSF fitting. Sequential cycles of photoactivation/localization/photobleaching are used to obtain the localization of each fluorophore in the structure and these coordinates are finally combined to reconstruct a super-resolution image (right panel). **(B)** PALM analysis of the spatial organization of RNA polymerase II (RNAP II) in mammalian cell nuclei. (i) By preconverting photoactivatable protein Dendra2 tagging RNAP II (green emission) before acquisition, conventional epifluorescence image can be obtained. (ii and iii) When performing stochastic photoactivation of RNAP II tagged with Dendra2 or the organic dye tetramethylrhodamine, a PALM (ii, red) or a STORM (iii, green) image reconstruction of the distribution of RNAP II can be obtained. iv depicts a zoomed-in area where individual STORM imaged transcription foci are discernible; yellow crosses indicate the centroid position of the clusters identified. Note that PALM and STORM imaging reveal the nonhomogeneous distribution of RNAP II in the cell nucleus. In (i) and (ii), white outlines represent an approximation of the nuclear contour. Scale bar in (i) and (ii) is 1 μm; in (iii) and (iv), the scale bar is 2 μm and 500 nm, respectively. **(C)** Resolution extension through the Moiré effect in structured illumination microscopy. The combination of sample information originating from structures below the diffraction limit with a known regular illumination pattern generates Moiré fringes. Exiting the sample with a known regular pattern in different orientations and processing all acquired images with complex computer algorithms generates a high-resolution image of the originally underlying structure. With this approach, the lateral resolution increases by a factor of two (120–150 nm depending on the illuminating wavelength, [99]). **(D)** Comparison of the resolution obtained by CLSM (left) and 3D SIM (right). At the bottom, zoom of details at the nuclear envelope. Nuclear pores (anti-NPC, red), nuclear envelope (anti-Lamin, green) and chromatin (DAPI-staining, blue). Scale bars: 1 μm. Figures in panels (B), (C), and (D) were reproduced with permission from [40,47,62,100]. Abbreviations: CLSM, confocal laser scanning microscopy; PALM, photo-activated localization microscopy; PSF, point-spread function; SIM, structured illumination microscopy; SRM, super-resolution microscopy; STORM, stochastic optical reconstruction microscopy.

Another method is to use organic fluorophores to label specific DNA-binding proteins or even the whole nucleus. Using chemical SNAP-tag labeling [44], live-cell dSTORM revealed the distribution of the core histone H2B on the nucleus with ~20 nm resolution [45,46], and Zhao *et al*. [47] obtained comparable results to those obtained by PALM for the RNA Pol II [40] (Figure 2B). Benke and Manley [48] took advantage of the photoswitching properties of a conventional

DNA staining agent to image the nucleus of U2OS cells at super-resolution. Similarly, Wang *et al*. [49] used binding activatable localization microscopy (BALM, [50]) to visualize chromatin fibers of ~400 nm in length and correlated decondensed chromatin regions with active transcription sites.

Despite the intrinsically slow acquisition rates of smSRM, the combination of this method with particle tracking provides unique information on the dynamic movement of single molecules within living cells. Single-particle tracking combined with photoactivation (usually termed spt-PALM) and single-molecule imaging technologies were used to track rapidly diffusing molecules and detect their binding to DNA [51,52], to understand the mechanisms by which transcription factors reach their target sites. These studies dissected the distinct exploration strategies of transcription factors in eukaryotes and bacteria and evaluated the role of DNA geometry on target-search kinetics [51,52]. Single-molecule imaging and tracking methods were also instrumental in studying the mechanisms of DNA repair [53] and in determining the diffusing or DNA-bound populations of condensin-like complexes in bacteria [54,55].

smSRM provides the highest spatial resolutions possible *in vivo*, but important limitations currently restrict its widespread use. 3D smSRM of thick samples is possible [56] but considerably increases the total acquisition time (to several hours per cell), whereas multicolor smSRM is currently limited due to the lack of bright, high-contrast, and stable fluorophores with nonoverlapping fluorescence emission spectra [57]. Very recent advances in multifocal plane microscopy combined with smSRM [58] and development and optimization of larger spectra fluorophores [59] may overcome many of these limitations.

Structured illumination microscopy (SIM)

SIM allows for 3D, multicolor imaging of cells with an eightfold improved volumetric resolution over conventional imaging (Figure 2C) [60,61]. The gain in spatial resolution of SIM is lower than that for smSRM (~120 nm versus ~20 nm in the lateral direction, respectively). However, SIM is often advantageous as it allows for considerably faster acquisition rates than smSRM (~10 s per 3D volume), permits the acquisition of multiple colors in 3D in a straightforward manner, and uses conventional fluorophores. SIM is thus the method of choice when faster, 3D, multicolor acquisitions are needed.

In a now classic study, Schermelleh *et al.*, [62] used SIM to probe the relative localization of DNA with respect to nuclear structures by simultaneously labeling chromatin with the DNA staining agent 4′,6-diamidino-2-phenylindole (DAPI), and nuclear lamina and nuclear pores by immunostaining. With this approach, the authors were able to show that nuclear pore complexes colocalized with channels in the lamin network and peripheral heterochromatin (Figure 2D), features unobserved previously by conventional microscopy approaches. In bacteria, SIM was used to investigate the mechanism by which molecular motors transfer DNA across membranes during cell division [43] and how DNA double-strand break (DSB) repair is carried out by the homologous recombination machinery [63].

To target genomic regions of DNA with high specificity, diverse techniques have been developed. For example, fluorescence *in situ* hybridization (FISH) labels can target genetic loci by annealing of complementary fluorescent DNA probes [64]. Recently, the combination of SIM and FISH allowed for the topographical analysis of defined nuclear targets [65]. Using this approach, van de Corput *et al*. [66] were able to study dynamic changes in chromatin structure of the β-globin locus of mouse cells to show that the 3D conformations of this locus changes in shape and volume upon cell differentiation. More recently, Giorgetti *et al.* [32] succeeded at labeling seven different loci at the interior of a single TAD of the mouse X chromosome and were able to correlate 3D spatial distance measurements with polymer model predictions based with 5C data, with astounding precision. These studies demonstrated that the internal chromatin conformation is correlated to differential transcription levels of individual loci within TADs.

In addition to a limited spatial resolution gain, SIM requires high-fluorescence intensity levels to obtain proper image reconstructions, can also produce high degrees of sample photobleaching, and is relatively slow (~10 s/vol) compared to many cellular processes. Thus, SIM is currently restricted to the study of bright structures displaying relatively slow dynamics. Cellular structures that photo bleach during acquisition tend to disappear in the final reconstructed image, while structures that move during the acquisition of the different angles/phases may lead to artifactual reconstructions. Several new improvements in SIM have recently allowed for considerably larger acquisition speeds and lower photobleaching rates, but at the expense of a decrease in spatial resolution [67,68]. Despite these limitations, future developments will likely make SIM the SRM of choice for many applications.

Fluorescence correlation methods

Fluorescence correlation spectroscopy (FCS) has been linked to the study of DNA since its first implementation [69]. Its development was initially limited due to technical reasons, but the advancement in laser technology, detector sensitivity, efficient computation, and improvement of fluorescent probes in the past 20 years has made FCS and its derived methodologies a widespread technique in most biophysical laboratories [70]. Single-point FCS allows for the study of single-molecule dynamics under equilibrium conditions with minimal perturbations both *in vivo* and *in vitro*. Its principle lies in the quantification of the magnitude and duration of fluorescent intensity fluctuations caused by molecules traveling through a small laser-illuminated volume (Figure 3A). From the fitting of a theoretical model to the autocorrelation function (ACF) of the fluorescence signal, the characteristic dwell time of the particles in the volume (i.e., their diffusion coefficient) and the concentration of the complexes under study can be obtained [71]. *In vivo*, variants of FCS (based on the scanning FCS principle, Figure 3A) allow for the exploration of larger areas in 2D (~10–100 μm^2) while conserving temporal resolutions below the microsecond and yield information such as density, concentration, aggregation, diffusion coefficients, velocities, and flow directions as well as interaction parameters [72,73].

The accessibility of chromatin to factors involved in transcription, DNA repair, and replication is tightly regulated by

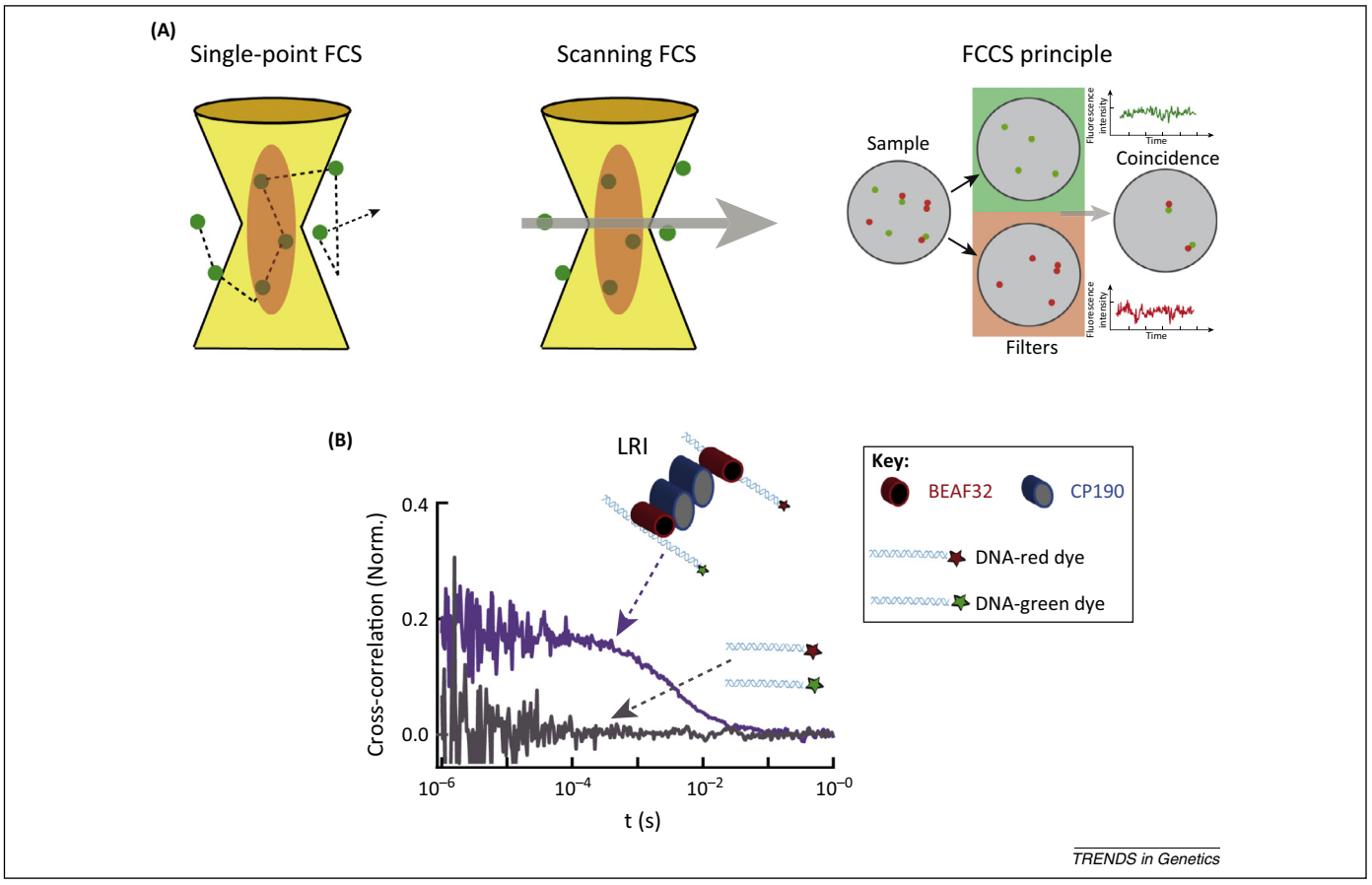

Figure 3. Correlation microscopy to study chromosomes structure and mechanisms. **(A)** Sketch of FCS and FCCS. In single-point FCS (left panel), molecules diffusing in and out of the excitation volume (red oval) are detected and recorded as a function of intensity versus time, whereas for scanning FCS (middle panel), each point of the line samples a different location (gray arrow) at a different time. If the particles move slowly with respect to the line-scanning time, at each point of the line we can observe intensity fluctuations. For FCCS experiments, a sample must contain molecules emitting in two colors (green and red dots). After passing through emission filters so that only one color is selected, the fluorescence fluctuation is measured by two independent detectors (see intensity vs. time traces in the side of each filter scheme). Only fluctuations that occur simultaneously in both channels due to the passage of the complex containing both molecules in the illumination volume contribute to the cross-correlation function (B) [101]. **(B)** Formation of LRI by insulator proteins studied by FCCS. After mixing dsDNA fragments labeled with either red or green fluorescent dyes (in the absence of insulator proteins) the autocorrelation function was estimated (gray solid line). Absence of cross-correlation is due to the lack of correlated movement of the two probes, and indicates that green and red-labeled dsDNA are not in the same molecular complex. When mixing the same DNAs but in presence of CP190 cofactor and the BEAF32 insulator protein, the positive cross-correlation signal at different times (violet solid line) indicates protein-mediated interactions between green- and red-labeled dsDNA. Figures in (A) and (B) were adapted from [80,101]. Abbreviations: BEAF, boundary element-associated factor; CP, centrosomal protein; dsDNA, double-stranded DNA; FCS, fluorescence correlation spectroscopy; FCCS, fluorescence cross-correlation spectroscopy; LRI, long-range interaction.

the epigenetic network. Using single-point FCS and raster image correlation spectroscopy (RICS), different groups have been able to reveal the dynamics of regulation of the different functional chromatin states (heterochromatin and euchromatin) by monitoring heterochromatin protein (HP)1 [72,74,75]. By using soluble, inert fluorescent probes of different sizes, it was shown that chromatin is spatially inhomogeneous [76] and displays a fractal organization [77]. Recently, by using a novel method combining micro-laser radiation to induce DNA breaks and the spatial pair cross-correlation function (pCF, [78]), Hinde and co-workers were able to monitor, by following the diffusion of EGFP in the millisecond time scale, the *in vivo* structural rearrangements of chromatin during DNA repair in HeLa cells [79]. The authors found that DNA damage is associated with a decrease of compaction at the damaged site concomitantly with a higher compaction at neighboring regions, suggesting that this combined mechanism facilitates the regulation and recruitment of repair factors to the lesion.

To further study molecular interactions, FCS can be extended to dual-color fluorescence cross-correlation spectroscopy (FCCS, Figure 3A). In FCCS, the molecules of interest are labeled with spectrally distinct fluorescent probes and from the correlation between the fluctuations of the different colors the cross-correlation function (CCF) is computed. Chromatin insulators are genetic elements implicated in nuclear organization and transcription regulation in eukaryotes via the formation of specific long-range interactions. To elucidate the minimal components and molecular mechanisms of insulator-mediated LRIs, Vogelmann *et al*. [80] used in *in vitro* FCCS. The authors reconstituted the minimal components of LRIs in *Drosophila* and were able to quantitatively determine whether two insulator elements belonged to the same molecular complex. Their results showed that the synergistic interaction between DNA-bound BEAF32 and CP190 is the key element in the establishment of strong and stable LRIs *in vitro* (Figure 3B). Similar FCCS approaches were used *in vivo* to study protein–protein interactions such as those of chromatin remodelers regulating gene expression [81].

Reliable FCS measurements depend on controlled and reproducible shape and dimensions of the focal volume. For accurate calibration, a bright and photostable reference sample with a known diffusion coefficient should be used.

Furthermore, the reference sample used for the focal volume estimation must be measured under the same conditions as those used for live cell experiments, as temperature significantly affects the estimation of diffusion times. FCCS data can be significantly altered by artifacts such as spectral crosstalk or misalignment of effective detection volumes of the two detection channels that will modify the apparent cross-correlation. Control experiments with negative (non-interacting molecules) and positive (molecules bearing both fluorophores) controls are needed to quantify interactions from cross-correlation amplitudes [82]. Incomplete labeling may also affect FCCS results as the characteristics of the binding events on a molecular level (e.g., stoichiometry and equilibrium binding constants) are obtained from the fraction of two-colored molecules in the complexes as determined from the ratio of the CCF amplitude to the ACF amplitude [83]. Measurements in living cells bring another level of complexity as refractive index mismatches between the cell constituents and surrounding media may affect the focal volume, while the cell autofluorescence, sample drift, cell movement, and photobleaching of the protein of interest may also impact the measurement. A current drawback of imaging FCS technologies is their reliance on reduced spatial resolution, as they are still limited by the optical diffraction limit [84]. Initial attempts of merging super-resolution and imaging correlation methods, although not yet applied to chromosome organization, show promising results [85,86].

Concluding remarks

Several disruptive technologies developed over the past decade have revolutionized our understanding of the 3D architecture of the chromosome. These various approaches each have their own limitations, but their rapid and diverse technological improvements will likely continue to shape this field in the near future.

One critical aspect of genomic 3C technologies is that it captures chromatin interactions of an ensemble of cells displaying different degrees of structural heterogeneity. This heterogeneity is due to many factors, including dynamics, cell cycle, presence of multiple chromosomes, or locus-specific structural changes coupled to specific activities (e.g., transcription). Many current developments aim at dissipating these sources of heterogeneity, by synchronizing cells, using haploid cell lines, or limiting dynamics by fixation. Critically, the further development of single-cell genomic 3C to concomitantly reach single-cell, high-throughput, and high-resolution contact maps could overcome many of these limitations. The use of single-cell Hi-C [33] combined with capture Hi-C [87] could already partially achieve these objectives. Together, these improvements in genomic 3C methods could lead to structural models of chromosome conformations based on structurally homogeneous datasets.

Such models would allow us to decipher the basic set of rules governing chromatin organization and regulation at the higher-order level. New emerging genomic engineering technologies such as RNA-guided endonucleases (RGENs) (Box 1) could enable the simultaneous modulation and localization of active genes. In addition, coupling genome editing and optogenetics could lead to the development of an inducible system capable of activating and deactivating gene expression with very fast kinetics at the single cell level. Recently developed optogenic gene expression technologies have shown promising results in this direction [88]. This method for locus-specific gene-expression manipulation, combined with imaging methods may permit the imaging of chromosome structures prior to and after light activation to determine the dynamics and architectural changes in chromatin induced by gene activation.

Several technical limitations thwart the use of super-resolution approaches to investigate chromosome structure and dynamics. First, these techniques are usually limited to a few colors (usually two, or three at best). Spectral imaging and linear unmixing may enable the simultaneous measurement of a large number of different probes (~10), therefore permitting the simultaneous detection of several markers at the single-cell level, including epigenetic marks, DNA (using Oligopaint probes, see below), and mRNA transcripts, etc. These simultaneous measurements would be instrumental in correlating chromosome architecture with its determinants and DNA management functions.

Second, current super-resolution methods are limited in penetration depth essentially due to out of focus light. Thus, measurements in specimens displaying large degrees of scattering are difficult. Recent advances in selective plane illumination microscopy (SPIM) [89] providing narrow excitation planes may considerably improve our ability to obtain super-resolved images in deep samples when combined with wide field super-resolution microscopies (PALM/STORM/SIM). Another difficulty of performing super-resolution imaging in deep specimens resides in the aberrations introduced by inhomogeneous media between the imaging plane and the objective. This problem may be circumvented by the use of adaptive optics [90,91] and by the optimization of biological sample preparation to reduce background noise and increase sample transparency (e.g., using models displaying low scattering in the visible spectrum). Together,

Box 1. Genome editing and chromosome architecture.

New emerging genomic engineering technologies could further revolutionize the field of chromatin structure and its relationship to genome activity by simultaneously allowing modulation and localization of active genes. Targeted genome engineering technologies (i.e., the modification of the genome at a precise, predetermined locus) such as RNA-guided engineered nucleases (RGENs, e.g., clustered, regularly interspaced, short palindromic repeat technology coupled to the Cas nucleases, CRISPR-Cas) use simple, base-pairing rules between an engineered RNA and the target DNA site allowing for great flexibility and customizable specificity [102,103]. With these technologies, synthetic chromosomes can be designed to address particular questions, for instance to unveil the mechanisms determining the *de novo* assembly of TADs and DNA loops. By introducing specific genes with different levels of expression or by exchanging natural promoters by repressible promoters and other similar strategies, the regulation of chromatin could be finely tuned externally, while changes in chromatin organization and architecture evaluated simultaneously by genome-wide and super-resolution microscopy. This kind of study could inform us about the role of active transcription in the formation of barriers between TADs. A second application of genome editing technologies involves the use of locus-specific labeling by fluorescently-tagged endonuclease-deficient proteins [104]. Extension of these strategies could soon enable the direct, *in vivo* labeling of extensive DNA regions to reach structural and dynamic information at the single-cell level using SRM. This specific development would enable the determination of heterogeneity and dynamics in the structures of a single TAD as well as the study of the mechanisms involved in establishing this structural heterogeneity.

these developments would permit the direct visualization of chromatin architecture in tissues or whole organisms (e.g., embryos), which will be essential to correlate chromatin structure to spatially-regulated development.

Third, direct imaging of whole chromosomes or higher-order chromosomal structures by super-resolution methods has been hampered by the lack of labeling strategies providing high-density and chemical specificity. Recently, a new technology termed Oligopaint [92] permitted the labeling of large genomic regions by the hybridization of short, single-stranded, fluorescently labeled DNA oligonucleotides containing a region of genomic homology. Libraries of varying sizes and densities can be designed depending on the labeling requirements. Recently, Oligopaint was coupled to super-resolution imaging to resolve previously unobserved morphologies for the BX-C locus in *Drosophila* cells [93]. The combination of these technologies with other developments to limit the degree of sample heterogeneity (e.g., cell cycle synchronization, and use of haploid cells) should provide a means to directly probe the spatial organization of different epigenetic chromatin domains at the single-cell level. These measurements, combined with locus-specific functional markers (e.g., for transcription, replication, or repair), will considerably improve our understanding of the interplay between chromosome organization and DNA management functions.

Finally, the 3D capability of the highest-resolution super-resolution methods (PALM/STORM) is limited to a depth of focus of $\sim 1\ \mu m$. This limitation is important as resolutions better than 50–100 nm are required to image higher-order chromatin structures (e.g., TADs and loops) and as the imaging of the whole nucleus is essential to correlate the localization of these structures to function. Initial attempts to address these issues using sequential scanning or two-photon excitation sources [56,94] have been limited by the long acquisition times required (~hours), photo-bleaching of planes located away from the imaging plane, and fluorophore availability. Recently, multifocus microscopy methods have enabled the instant acquisition of whole cellular volumes at super-resolution [58,95]. Improvements in the efficiency of light collection in this technology, combined with SPIM could in the future provide a means to obtain full nucleoid, multicolor, super-resolution images of higher-order chromatin structures.

Despite these challenges, genomic 3C and advanced microscopy methods have already lead to a re-evaluation of many established concepts in chromatin biology. The current pace of new developments in these technologies can only augur new revolutions to come.

Acknowledgments

We acknowledge support for this work to the European Research Council under the 7th Framework Program (FP7/2010-2015) to M.N. (ERC grant agreement 260787).

References

1 Misteli, T. (2010) Higher-order genome organization in human disease. *Cold Spring Harb. Perspect. Biol.* 2, a000794
2 Bolzer, A. *et al.* (2005) Three-dimensional maps of all chromosomes in human male fibroblast nuclei and prometaphase rosettes. *PLoS Biol.* 3, e157
3 Cremer, T. *et al.* (2006) Chromosome territories – a functional nuclear landscape. *Curr. Opin. Cell Biol.* 18, 307–316
4 Lanctot, C. *et al.* (2007) Dynamic genome architecture in the nuclear space: regulation of gene expression in three dimensions. *Nat. Rev. Genet.* 8, 104–115
5 Haarhuis, J.H. *et al.* (2014) Cohesin and its regulation: on the logic of X-shaped chromosomes. *Dev. Cell* 31, 7–18
6 Postow, L. *et al.* (2004) Topological domain structure of the *Escherichia coli* chromosome. *Genes Dev.* 18, 1766–1779
7 Espeli, O. *et al.* (2008) DNA dynamics vary according to macrodomain topography in the E. coli chromosome. *Mol. Microbiol.* 68, 1418–1427
8 de Wit, E. and de Laat, W. (2012) A decade of 3C technologies: insights into nuclear organization. *Genes Dev.* 26, 11–24
9 Dostie, J. *et al.* (2006) Chromosome Conformation Capture Carbon Copy (5C): a massively parallel solution for mapping interactions between genomic elements. *Genome Res.* 16, 1299–1309
10 Lieberman-Aiden, E. *et al.* (2009) Comprehensive mapping of long-range interactions reveals folding principles of the human genome. *Science* 326, 289–293
11 Sexton, T. *et al.* (2012) Three-dimensional folding and functional organization principles of the *Drosophila* genome. *Cell* 148, 458–472
12 Ma, W. *et al.* (2015) Fine-scale chromatin interaction maps reveal the cis-regulatory landscape of human lincRNA genes. *Nat. Methods* 12, 71–78
13 Nora, E.P. *et al.* (2012) Spatial partitioning of the regulatory landscape of the X-inactivation centre. *Nature* 485, 381–385
14 Dixon, J.R. *et al.* (2012) Topological domains in mammalian genomes identified by analysis of chromatin interactions. *Nature* 485, 376–380
15 Hou, C. *et al.* (2012) Gene density, transcription, and insulators contribute to the partition of the *Drosophila* genome into physical domains. *Mol. Cell* 48, 471–484
16 Nora, E.P. *et al.* (2013) Segmental folding of chromosomes: a basis for structural and regulatory chromosomal neighborhoods? *Bioessays* 35, 818–828
17 Sanyal, A. *et al.* (2012) The long-range interaction landscape of gene promoters. *Nature* 489, 109–113
18 Jin, F. *et al.* (2013) A high-resolution map of the three-dimensional chromatin interactome in human cells. *Nature* 503, 290–294
19 Rao, S.S. *et al.* (2014) A 3D map of the human genome at kilobase resolution reveals principles of chromatin looping. *Cell* 159, 1665–1680
20 Dekker, J. *et al.* (2013) Exploring the three-dimensional organization of genomes: interpreting chromatin interaction data. *Nat. Rev. Genet.* 14, 390–403
21 Collas, P. and Dahl, J.A. (2008) Chop it, ChIP it, check it: the current status of chromatin immunoprecipitation. *Front. Biosci.* 13, 929–943
22 Wold, B. and Myers, R.M. (2008) Sequence census methods for functional genomics. *Nat. Methods* 5, 19–21
23 Pope, B.D. *et al.* (2014) Topologically associating domains are stable units of replication-timing regulation. *Nature* 515, 402–405
24 Naumova, N. *et al.* (2013) Organization of the mitotic chromosome. *Science* 342, 948–953
25 Comet, I. *et al.* (2011) A chromatin insulator driving three-dimensional Polycomb response element (PRE) contacts and Polycomb association with the chromatin fiber. *Proc. Natl. Acad. Sci. U.S.A.* 108, 2294–2299
26 Umbarger, M.A. *et al.* (2011) The three-dimensional architecture of a bacterial genome and its alteration by genetic perturbation. *Mol. Cell* 44, 252–264
27 Cagliero, C. *et al.* (2013) Genome conformation capture reveals that the *Escherichia coli* chromosome is organized by replication and transcription. *Nucleic Acids Res.* 41, 6058–6071
28 Marbouty, M. *et al.* (2014) Metagenomic chromosome conformation capture (meta3C) unveils the diversity of chromosome organization in microorganisms. *Elife* 3, e03318
29 Le, T.B. *et al.* (2013) High-resolution mapping of the spatial organization of a bacterial chromosome. *Science* 342, 731–734
30 Lajoie, B.R. *et al.* (2015) The Hitchhiker's guide to Hi-C analysis: practical guidelines. *Methods* 72, 65–75
31 Gavrilov, A. *et al.* (2014) In vivo formaldehyde cross-linking: it is time for black box analysis. *Brief Funct. Genomics* 14, 163–165
32 Giorgetti, L. *et al.* (2014) Predictive polymer modeling reveals coupled fluctuations in chromosome conformation and transcription. *Cell* 157, 950–963
33 Nagano, T. *et al.* (2013) Single-cell Hi-C reveals cell-to-cell variability in chromosome structure. *Nature* 502, 59–64

34 Betzig, E. *et al.* (2006) Imaging intracellular fluorescent proteins at nanometer resolution. *Science* 313, 1642–1645
35 Hess, S.T. *et al.* (2006) Ultra-high resolution imaging by fluorescence photoactivation localization microscopy. *Biophys. J.* 91, 4258–4272
36 Rust, M.J. *et al.* (2006) Sub-diffraction-limit imaging by stochastic optical reconstruction microscopy (STORM). *Nat. Methods* 3, 793–795
37 Heilemann, M. *et al.* (2009) Super-resolution imaging with small organic fluorophores. *Angew. Chem. Int. Ed. Engl.* 48, 6903–6908
38 Heilemann, M. *et al.* (2008) Subdiffraction-resolution fluorescence imaging with conventional fluorescent probes. *Angew. Chem. Int. Ed. Engl.* 47, 6172–6176
39 Fernandez-Suarez, M. and Ting, A.Y. (2008) Fluorescent probes for super-resolution imaging in living cells. *Nat. Rev. Mol. Cell Biol.* 9, 929–943
40 Cisse, I. *et al.* (2013) Real-time dynamics of RNA polymerase II clustering in live human cells. *Science* 341, 664–667
41 Wang, W. *et al.* (2011) Chromosome organization by a nucleoid-associated protein in live bacteria. *Science* 333, 1445–1449
42 Wang, S. *et al.* (2014) Characterization and development of photoactivatable fluorescent proteins for single-molecule-based superresolution imaging. *Proc. Natl. Acad. Sci. U.S.A.* 111, 8452–8457
43 Fiche, J-B. *et al.* (2013) Recruitment, assembly, and molecular architecture of the SpoIIIE DNA pump revealed by superresolution microscopy. *PLoS Biol.* 11, e1001557
44 Keppler, A. *et al.* (2003) A general method for the covalent labeling of fusion proteins with small molecules in vivo. *Nat. Biotechnol.* 21, 86–89
45 Wombacher, R. *et al.* (2010) Live-cell super-resolution imaging with trimethoprim conjugates. *Nat. Methods* 7, 717–719
46 Klein, T. *et al.* (2011) Live-cell dSTORM with SNAP-tag fusion proteins. *Nat. Methods* 8, 7–9
47 Zhao, Z.W. *et al.* (2014) Spatial organization of RNA polymerase II inside a mammalian cell nucleus revealed by reflected light-sheet superresolution microscopy. *Proc. Natl. Acad. Sci. U.S.A.* 111, 681–686
48 Benke, A. and Manley, S. (2012) Live-cell dSTORM of cellular DNA based on direct DNA labeling. *Chembiochem* 13, 298–301
49 Wang, Y. *et al.* (2014) Super-resolution microscopy reveals decondensed chromatin structure at transcription sites. *Sci. Rep.* 4, 4477
50 Schoen, I. *et al.* (2011) Binding-activated localization microscopy of DNA structures. *Nano Lett.* 11, 4008–4011
51 Izeddin, I. *et al.* (2014) Single-molecule tracking in live cells reveals distinct target-search strategies of transcription factors in the nucleus. *Elife* 3, e02230
52 Hammar, P. *et al.* (2012) The lac repressor displays facilitated diffusion in living cells. *Science* 336, 1595–1598
53 Uphoff, S. *et al.* (2013) Single-molecule DNA repair in live bacteria. *Proc. Natl. Acad. Sci. U.S.A.* 110, 8063–8068
54 Badrinarayanan, A. *et al.* (2012) In vivo architecture and action of bacterial structural maintenance of chromosome proteins. *Science* 338, 528–531
55 Kleine Borgmann, L.A. *et al.* (2013) The bacterial SMC complex displays two distinct modes of interaction with the chromosome. *Cell Rep.* 3, 1483–1492
56 York, A.G. *et al.* (2011) Confined activation and subdiffractive localization enables whole-cell PALM with genetically expressed probes. *Nat. Methods* 8, 327–333
57 Nienhaus, K. and Nienhaus, G.U. (2014) Fluorescent proteins for live-cell imaging with super-resolution. *Chem. Soc. Rev.* 43, 1088–1106
58 Hajj, B. *et al.* (2014) Whole-cell, multicolor superresolution imaging using volumetric multifocus microscopy. *Proc. Natl. Acad. Sci. U.S.A.* 111, 17480–17485
59 Grimm, J.B. *et al.* (2015) A general method to improve fluorophores for live-cell and single-molecule microscopy. *Nat. Methods* 12, 244–250
60 Gustafsson, M.G. (2000) Surpassing the lateral resolution limit by a factor of two using structured illumination microscopy. *J. Microsc.* 198, 82–87
61 Gustafsson, M.G.L. *et al.* (2008) Three-dimensional resolution doubling in wide-field fluorescence microscopy by structured illumination. *Biophys. J.* 94, 4957–4970
62 Schermelleh, L. *et al.* (2008) Subdiffraction multicolor imaging of the nuclear periphery with 3D structured illumination microscopy. *Science* 320, 1332–1336
63 Lesterlin, C. *et al.* (2014) RecA bundles mediate homology pairing between distant sisters during DNA break repair. *Nature* 506, 249–253
64 Langer-Safer, P.R. *et al.* (1982) Immunological method for mapping genes on *Drosophila* polytene chromosomes. *Proc. Natl. Acad. Sci. U.S.A.* 79, 4381–4385
65 Markaki, Y. *et al.* (2012) The potential of 3D-FISH and super-resolution structured illumination microscopy for studies of 3D nuclear architecture: 3D structured illumination microscopy of defined chromosomal structures visualized by 3D (immuno)-FISH opens new perspectives for studies of nuclear architecture. *Bioessays* 34, 412–426
66 van de Corput, M.P. *et al.* (2012) Super-resolution imaging reveals three-dimensional folding dynamics of the beta-globin locus upon gene activation. *J. Cell Sci.* 125, 4630–4639
67 York, A.G. *et al.* (2012) Resolution doubling in live, multicellular organisms via multifocal structured illumination microscopy. *Nat. Methods* 9, 749–754
68 York, A.G. *et al.* (2013) Instant super-resolution imaging in live cells and embryos via analog image processing. *Nat. Methods* 10, 1122–1126
69 Magde, D. *et al.* (1972) Thermodynamic fluctuations in a reacting system – measurement by fluorescence correlation spectroscopy. *Phys. Rev. Lett.* 29, 705–708
70 Chen, H. *et al.* (2008) In vivo applications of fluorescence correlation spectroscopy. In *Methods in Cell Biology* (John, J.C. and Detrich, H.C., eds), pp. 3–35, Academic Press
71 Saffarian, S. and Elson, E.L. (2003) Statistical analysis of fluorescence correlation spectroscopy: the standard deviation and bias. *Biophys. J.* 84, 2030–2042
72 Erdel, F. *et al.* (2011) Dissecting chromatin interactions in living cells from protein mobility maps. *Chromosome Res.* 19, 99–115
73 Annibale, P. and Gratton, E. (2014) Advanced fluorescence microscopy methods for the real-time study of transcription and chromatin dynamics. *Transcription* 5, e28425
74 Muller, K.P. *et al.* (2009) Multiscale analysis of dynamics and interactions of heterochromatin protein 1 by fluorescence fluctuation microscopy. *Biophys J.* 97, 2876–2885
75 Hemmerich, P. *et al.* (2011) Dynamic as well as stable protein interactions contribute to genome function and maintenance. *Chromosome Res.* 19, 131–151
76 Dross, N. *et al.* (2009) Mapping eGFP oligomer mobility in living cell nuclei. *PLoS ONE* 4, e5041
77 Bancaud, A. *et al.* (2009) Molecular crowding affects diffusion and binding of nuclear proteins in heterochromatin and reveals the fractal organization of chromatin. *EMBO J.* 28, 3785–3798
78 Digman, M.A. and Gratton, E. (2009) Imaging barriers to diffusion by pair correlation functions. *Biophys. J.* 97, 665–673
79 Hinde, E. *et al.* (2014) Chromatin dynamics during DNA repair revealed by pair correlation analysis of molecular flow in the nucleus. *Biophys. J.* 107, 55–65
80 Vogelmann, J. *et al.* (2014) Chromatin insulator factors involved in long-range DNA interactions and their role in the folding of the *Drosophila* genome. *PLoS Genet.* 10, e1004544
81 Siegel, A.P. *et al.* (2013) Unraveling transcription factor interactions with heterochromatin protein 1 using fluorescence lifetime imaging microscopy and fluorescence correlation spectroscopy. *J. Biomed. Opt.* 18, 25002
82 Machan, R. and Wohland, T. (2014) Recent applications of fluorescence correlation spectroscopy in live systems. *FEBS Lett.* 588, 3571–3584
83 Foo, Y.H. *et al.* (2012) Factors affecting the quantification of biomolecular interactions by fluorescence cross-correlation spectroscopy. *Biophys. J.* 102, 1174–1183
84 Bag, N. and Wohland, T. (2014) Imaging fluorescence fluctuation spectroscopy: new tools for quantitative bioimaging. *Annu. Rev. Phys. Chem.* 65, 225–248
85 Eggeling, C. *et al.* (2009) Direct observation of the nanoscale dynamics of membrane lipids in a living cell. *Nature* 457, 1159–1162
86 Hedde, P.N. *et al.* (2013) Stimulated emission depletion-based raster image correlation spectroscopy reveals biomolecular dynamics in live cells. *Nat. Commun.* 4, 2093
87 Mifsud, B. *et al.* (2015) Mapping long-range promoter contacts in human cells with high-resolution capture Hi-C. *Nat. Genetics* 47, 598–606

88 Motta-Mena, L.B. *et al.* (2014) An optogenetic gene expression system with rapid activation and deactivation kinetics. *Nat. Chem. Biol.* 10, 196–202
89 Chen, B.C. *et al.* (2014) Lattice light-sheet microscopy: imaging molecules to embryos at high spatiotemporal resolution. *Science* 346, 1257998
90 Izeddin, I. *et al.* (2012) PSF shaping using adaptive optics for three-dimensional single-molecule super-resolution imaging and tracking. *Opt. Express* 20, 4957–4967
91 Gould, T.J. *et al.* (2012) Adaptive optics enables 3D STED microscopy in aberrating specimens. *Opt Express* 20, 20998–21009
92 Beliveau, B.J. *et al.* (2012) Versatile design and synthesis platform for visualizing genomes with Oligopaint FISH probes. *Proc. Natl. Acad. Sci. U.S.A.* 109, 21301–21306
93 Beliveau, B.J. *et al.* (2015) Single-molecule super-resolution imaging of chromosomes and in situ haplotype visualization using Oligopaint FISH probes. *Nat. Commun.* 6, 7147–7151
94 Vaziri, A. *et al.* (2008) Multilayer three-dimensional super resolution imaging of thick biological samples. *Proc. Natl. Acad. Sci. U.S.A.* 105, 20221–20226
95 Abrahamsson, S. *et al.* (2013) Fast multicolor 3D imaging using aberration-corrected multifocus microscopy. *Nat. Methods* 10, 60–63
96 Sanyal, A. *et al.* (2011) Chromatin globules: a common motif of higher order chromosome structure? *Curr. Opin. Cell Biol.* 23, 325–331
97 Mundade, R. *et al.* (2014) Role of ChIP-seq in the discovery of transcription factor binding sites, differential gene regulation mechanism, epigenetic marks and beyond. *Cell Cycle* 13, 2847–2852
98 Bantignies, F. *et al.* (2011) Polycomb-dependent regulatory contacts between distant Hox loci in *Drosophila*. *Cell* 144, 214–226
99 Schermelleh, L. *et al.* (2010) A guide to super-resolution fluorescence microscopy. *J. Cell Biol.* 190, 165–175
100 Gustafsson, M.G. (2005) Nonlinear structured-illumination microscopy: wide-field fluorescence imaging with theoretically unlimited resolution. *Proc. Natl. Acad. Sci. U.S.A.* 102, 13081–13086
101 Digman, M.A. and Gratton, E. (2011) Lessons in fluctuation correlation spectroscopy. *Annu. Rev. Phys. Chem.* 62, 645–668
102 Cho, S.W. *et al.* (2013) Targeted genome engineering in human cells with the Cas9 RNA-guided endonuclease. *Nat. Biotechnol.* 31, 230–232
103 Cong, L. *et al.* (2013) Multiplex genome engineering using CRISPR/Cas systems. *Science* 339, 819–823
104 Chen, B. *et al.* (2013) Dynamic imaging of genomic loci in living human cells by an optimized CRISPR/Cas system. *Cell* 155, 1479–1491